Optics Letters

Uncloaking diffusive-light invisibility cloaks by speckle analysis

Andreas Niemeyer,[1,*] Frederik Mayer,[1,2] Andreas Naber,[1] Milan Koirala,[3] Alexey Yamilov,[3] and Martin Wegener[1,2]

[1]Institute of Applied Physics, Karlsruhe Institute of Technology (KIT), Karlsruhe 76128, Germany
[2]Institute of Nanotechnology, Karlsruhe Institute of Technology (KIT), Karlsruhe 76021, Germany
[3]Physics Department, Missouri University of Science and Technology, Rolla, Missouri 65409, USA
*Corresponding author: Andreas.Niemeyer@kit.edu

Received 25 January 2017; accepted 8 April 2017; posted 21 April 2017 (Doc. ID 285550); published 12 May 2017

Within the range of validity of the stationary diffusion equation, an ideal diffusive-light invisibility cloak can make an arbitrary macroscopic object hidden inside of the cloak indistinguishable from the surroundings for all colors, polarizations, and directions of incident visible light. However, the diffusion equation for light is an approximation which becomes exact only in the limit of small coherence length. Thus, one expects that the cloak can be revealed by illumination with coherent light. The experiments presented here show that the cloaks are robust in the limit of large coherence length but can be revealed by analysis of the speckle patterns under illumination with partially coherent light. Experiments on cylindrical core-shell cloaks and corresponding theory are in good agreement.

OCIS codes: (230.3205) Invisibility cloaks; (290.1990) Diffusion; (290.4210) Multiple scattering; (290.5839) Scattering, invisibility.

https://doi.org/10.1364/OL.42.001998

The purpose of any cloak is to make an arbitrary object hidden inside of the cloak indistinguishable from the surroundings with respect to some observable feature [1]. A specific cloak works for a specific surrounding only. For example, in water or in a cloud, an optical invisibility cloak designed for vacuum or air would appear as a void and would hence be visible. Broadly speaking, cloaking can be seen as a striking example for which the corresponding tomography problem does not have a unique solution [2].

With respect to invisibility cloaking for electromagnetic waves following the Maxwell equations for continua, fundamental limitations of cloaking [3–5] and possibilities to uncloak the cloak have been discussed in detail. For example, due to relativity, a macroscopic object can be hidden only for a relatively small part of the electromagnetic spectrum. [4]. The extinction cross section of the cloak, integrated over all frequencies, is always larger than that of the object to be hidden alone [5]. The cloak can be uncloaked by Cherenkov radiation of charged particles passing through the cloak [6], or by motion of the cloak with respect to the source and observer at relativistic speeds [7].

The situation is less clear in regard to invisibility cloaking in turbid media, where light propagation follows a diffusion equation [8,9]. Ideal cloaks can be designed by using coordinate transformations [10], and approximate cloaks have been realized by simplified core-shell structures [11–13]. Homogenizing the light emission from Lambertian emitters such as organic light-emitting diodes (OLEDs) with shadowing metal contacts on top is a possible application [14]. Conceptually, diffusive cloaking of macroscopic objects can be ideal for the entire visible spectrum and for all polarizations and directions of incident light—at least for stationary or quasi-stationary [15–17] conditions. It is thus interesting to also investigate fundamental limitations of diffusive-light cloaking, allowing for revealing the cloaks—which is the aim of the present work.

It is clear that the diffusion equation does not account for coherent wave effects like, e.g., speckles [8]. All previous experiments on core-shell structures have used illumination with incoherent white light [11–13]. Experiments in the opposite limit of illumination with coherent light from a continuous-wave laser (Toptica, DL100) operating at around $\lambda = 780$ nm wavelength along the positive z direction are depicted in Fig. 1. The bandwidth of this laser is less than 5 MHz, corresponding to a coherence length in air exceeding 60 m. The behavior shown in Fig. 1 is similar to the one for illumination with incoherent white light [12]: the obstacle casts a pronounced diffusive shadow, which essentially disappears for the cloak sample, making it indistinguishable from the reference. For all samples, pronounced spatial intensity fluctuations, i.e., speckles, are superimposed. Altogether, the cloak cannot be revealed by such an experiment.

Here, we use the same samples as in our previous work [12]: the cuboid reference sample with dimensions $L_x = 15$ cm, $L_y = 8$ cm, and $L_z = 3$ cm contains a constant density of TiO_2 nanoparticles (DuPont, R700) with an average diameter of 340 nm within a homogeneous and transparent polydimethylsiloxane (PDMS) matrix, leading to an effective light diffusivity of $D_0 = 11.9 \times 10^8$ cm^2 s^{-1} [12]. The corresponding

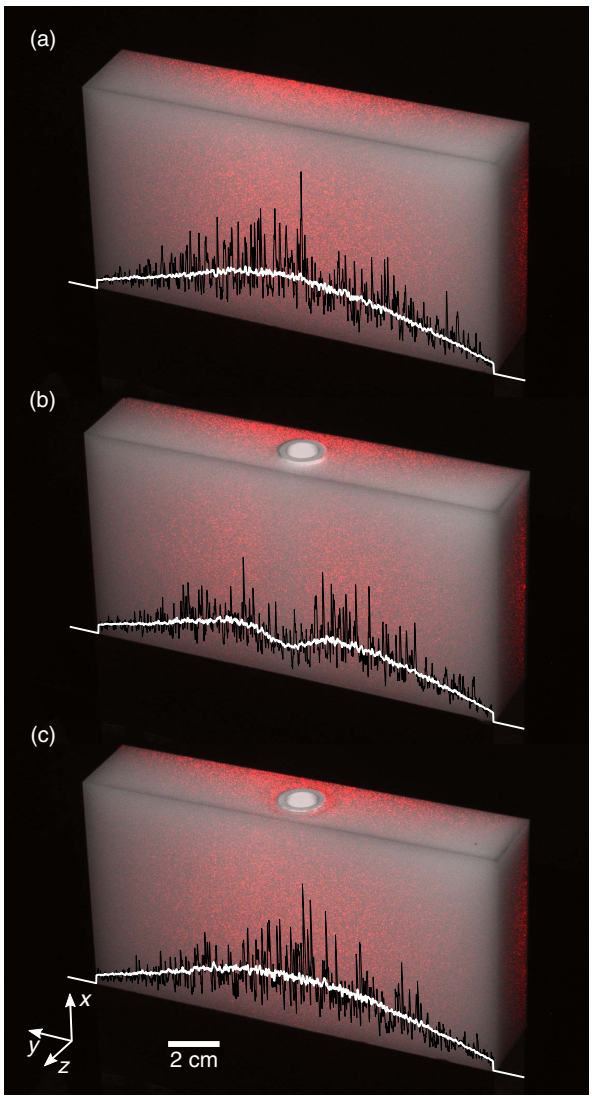

Fig. 1. Images of (a) the reference, (b) the obstacle, and (c) the cloak sample under large-area illumination from the rear side (i.e., along the positive z direction) with coherent laser light at $\lambda = 780$ nm wavelength (red). No polarizer is used in front of the camera. Each image results from two exposures: one with white-light illumination to reveal the sample and one with laser illumination. The laser light leads to strong intensity fluctuations (speckles). The two images are superimposed in the computer. The black curves are intensity cuts through the middle of the samples, projected onto the sample's surface. The white curves show the intensity averaged along the vertical direction from 25% to 75% of the sample height. We find that the obstacle casts a diffuse shadow, which essentially disappears for the cloak, making it indistinguishable from the reference. This overall behavior for illumination with coherent light is closely similar to that for illumination with incoherent white light, which we have published previously [12].

transport mean free path length is $l_t^0 = 1.67$ mm. The scattering mean free path length of $l_s^0 = 0.76$ mm $= l_t^0 \times (1 - \langle \cos\theta \rangle)$ has been measured independently [12] and leads to an asymmetry value of $g = \langle \cos\theta \rangle = 0.544$ [13]. This value indicates preferential forward scattering, which is expected for TiO_2 nanoparticles of this size. The obstacle sample additionally contains a hollow cylindrical ceramic core (Accuratus Corporation, Accuflect B6) in the center of the xz plane, with the cylinder axis parallel to the y axis. It has an outer radius of $R_1 = 0.8$ cm and acts as a Lambertian diffusive reflector with diffusivity $D_1 \ll D_0$. The cloak sample contains an additional PDMS cylindrical shell with outer radius $R_2 = 1.2$ cm $= 1.5 \times R_1$ around the core. The shell is doped with a 3.9 times lower concentration of TiO_2 nanoparticles than the surroundings, leading to a light diffusivity of $D_2 = 3.9 \times D_0$ [12]. Arbitrary objects can be placed into the opaque hollow ceramic core, qualifying the arrangement as a true cloak rather than just as an invisible object.

The mean distance between the intensity peaks of the speckle patterns in Fig. 1 is mainly determined by the resolution capability of the imaging system. To better resolve the speckles, we perform additional experiments. We illuminate the center of the rear side of the sample (parallel to the xy plane) with a collimated Gaussian beam (with about 2 mm diameter) of the same laser impinging along the positive z direction. We image only a small region with about 1 mm^2 footprint in the center of the sample's front side by using a single microscope objective lens (Olympus, 605339, 10×, NA = 0.25) and a charge-coupled-device (CCD) grayscale silicon camera (Point Grey, BFLY-PGE-50H5M-C, 12 bits dynamic range). To maximize the effects and to obtain good statistics, we have chosen this region to be small compared to the cloak diameter and large compared to the speckle size. In contrast to Fig. 1, a linear polarizer is located in front of the camera; without the polarizer, one would obtain an incoherent superposition of two independent speckle patterns. The speckle contrast is defined as $C_I = \sigma_I / \langle I \rangle$, with the standard deviation of the intensity pattern σ_I and the average intensity I. The measured camera images contain the effects of electrical noise. We thus first subtract a dark image I_{ij}^0, i.e., $I_{ij} \to I_{ij} - I_{ij}^0$. Negative values I_{ij} can result. We then compute the average $I = N^{-1} \sum_{ij} I_{ij}$ and the intensity standard deviation $\sigma_I = N^{-1} \sum_{ij} (I_{ij} - I)^2$, with the number of camera pixels $N = 2448 \times 2048$. The camera exposure time is adjusted such that pixel values much larger than $\langle I \rangle$ are still below the saturation value I_{sat}, i.e., $I = I_{sat}/15$. Otherwise, the speckle statistics could be distorted. The measured speckle contrast is equal to within the error bars for reference and cloak, respectively, and typically around $C_I = 95\%$ in both cases [see Fig. 2(b)]. This value is close to the expected theoretical ideal of $C_I = 100\%$ for fully coherent speckles from scattering off bulk turbid media or surfaces [8]. The 5% difference can be traced back to electrical noise, which smears out the contrast despite the above-mentioned background subtraction. Importantly, the cloak *cannot* be revealed in this manner.

To reveal the cloak, recent theoretical work [18] has suggested computing the long-range contribution of the second-order intensity correlation function C_2[19] from such speckle patterns for fully coherent illumination. It relies on the existence of crossings and interference of diffusive paths. Occurrence of such processes has low probability in our highly diffusive system with $l_t^0 \gg \lambda$. Indeed, the published formulas applied to our sample parameters yield that the peak relative differences between reference and cloak are expected to be on the order of merely

$$|\Delta C_2^{\max}| \approx \frac{1}{2} \frac{\lambda}{l_t^0} \frac{R_2^2}{L_z^2} \approx 4 \times 10^{-5}$$

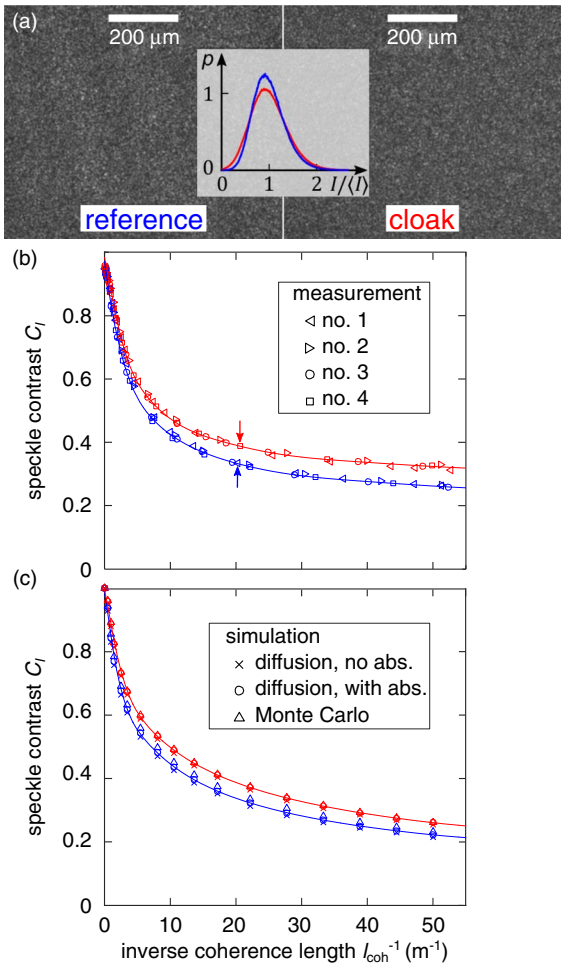

Fig. 2. In contrast to Fig. 1, only the center of the rear side of the sample is illuminated with a narrow beam, and a linear polarizer is placed in front of the camera. Furthermore, illumination is with partially coherent light with adjustable effective coherence length l_{coh}. (a) One example [$l_{\mathrm{coh}} = 4.8$ cm, see arrows in (b)] of a resolved measured speckle image for a magnified view onto the center of the front side of the reference (left) and the cloak sample (right). The inset shows the corresponding histograms, normalized to unity integral, versus normalized intensity $I/\langle I\rangle$. (b) Derived speckle contrast, C_I, versus inverse coherence length l_{coh}^{-1} for the reference (blue) and the cloak (red) sample. The solid curves are guides to the eye. (c) Calculated speckle contrast versus l_{coh}^{-1} represented as the experiments in (b). The different symbols correspond to diffusion theory without absorption (crosses), diffusion theory with absorption (circles), and Monte Carlo ray-tracing simulations (triangles).

for $\lambda = 780$ nm. Such small relative differences are very difficult to resolve for realistic statistics and signal-to-noise ratios. Thus, in practice, the cloaks discussed here cannot be revealed in this manner either.

The diffusive-light cloak works well for incoherent illumination as well as for coherent illumination. Can it be revealed for the intermediate case of partially coherent illumination?

It is known from our time-resolved measurements [13,15] that the propagation-time distributions are different for reference and cloak. The propagation time, t, distribution can be converted into a path-length distribution $P(s)$, with $s = c\,t$ and the medium velocity of light c. The distribution $P(s)$ could alternatively be measured by an interferometric approach [20]. The physical reason for the different path-length distributions $P(s)$ is that the cloaking shell has a larger diffusivity of light than the surroundings to compensate for the near-zero diffusivity of the core. The diffusion time is inversely proportional to the diffusivity and determines the width of the path-length distribution, which is thus larger for the reference than for the cloak. This trend is partly compensated for by the fact that light has to make a detour around the core and that part of the propagation is in the surrounding medium for the cloak sample.

References [21–23] describe an experimental approach based on measuring speckle contrast for illumination with partially coherent light to obtain certain information about $P(s)$ without actually determining the entire path-length distribution via demanding time-resolved or interferometric measurements. This approach has previously been employed for studying the internal microscopic structure of a scattering medium [24], detection of buried objects [22], and imaging in biomedical optics [25]. It is however, not *a priori* clear whether such measurement can recover enough information to reveal the existence of a cloaked object.

To test this idea, we have performed experiments in which we sweep the center frequency of the laser [monitored by a Fabry–Perot interferometer (Toptica, FPI 780)] in a periodic triangular temporal pattern, leading to a box-shaped spectrum of frequency width Δf. The camera exposure time of 250 ms is chosen to be large compared to the sweep period of 4 ms, such that this spectral width Δf effectively corresponds to a coherence length in air given by $l_{\mathrm{coh}} = c_0/\Delta f$, with the vacuum speed of light c_0. Figure 2 exhibits the measured speckle contrast of the reference (blue curve) and the cloak (red curve) samples versus the inverse coherence length; Fig. 2(a) depicts examples of underlying raw data. To test the reproducibility, we have repeated the experiments on different days and have intentionally taken the samples in and out of the setup in between [see measurements no. 1–4 in Fig. 2(b)]. We find the cloak behaves significantly and systematically different from the reference for intermediate coherence lengths. If no separate reference sample should be available, the observer could equivalently compare the speckle contrast of images centered at the cloak position and horizontally separated from the center by a few times the diameter or the depth of the cloak (whichever is larger). This finding means that the cloak can indeed be uncloaked using partially coherent illumination, while the cloak works well for very small coherence lengths (white-light illumination, see [12]) as well as for very large coherence lengths.

To test the validity of our interpretation, we have performed corresponding theoretical calculations. Mathematically, the speckle contrast can be obtained [21] from

$$C_I = \frac{\left[\int_0^\infty \int_0^\infty \mathcal{S}(\lambda)\mathcal{S}(\lambda')F(\lambda,\lambda')\mathrm{d}\lambda\mathrm{d}\lambda'\right]^{\frac{1}{2}}}{\int_0^\infty \mathcal{S}(\lambda)\mathrm{d}\lambda}. \quad (1)$$

The contrast depends on the spectral profile $\mathcal{S}(\lambda)$ and the distribution of path lengths $P(s)$ via the function

$$F(\lambda,\lambda') = \left|\int_0^\infty P(s)\exp[2\pi\mathrm{i}\, s(\lambda^{-1} - \lambda'^{-1})]\mathrm{d}s\right|^2, \quad (2)$$

which is essentially a Fourier transform of $P(s)$. In our case, the spectral profile is a rectangular function with a width defined by

l_{coh}. It can be shown that $l_{coh} \to \infty \Rightarrow C_I \to 1$ and $l_{coh} \to 0 \Rightarrow C_I \propto \sqrt{l_{coh}/\Delta s}$, with the width of the path-length distribution Δs. While Δs is different for reference and cloak, $C_I \to 0$ holds true for both, i.e., the cloak cannot be revealed using incoherent light. For partially coherent light, the only remaining input is the path-length distribution $P(s)$ that we compute using two different numerical methods: (i) solution of the diffusion equation [13] or (ii) Monte Carlo simulations [13]. In the case of the reference sample, both methods agree well, whereas we observe slight differences in $P(s)$ for the case of the cloak sample. This finding is due to the fact that the thickness of the cloak is not much larger than the transport mean free path and, therefore, the Monte Carlo approach should provide a more accurate description of light propagation.

The results of numerical evaluation of Eqs. (1) and (2), shown in Fig. 2(c), reproduce the measurements shown in Fig. 2(b) well. In particular, we observe an onset of modification of the speckle contrast when l_{coh}/c_0 becomes comparable to the time of diffusive light propagation through the sample [26] $\tau_{diff} = L_z^2/6D_0 \approx 1.3$ ns, which translates into $l_{coh}^{-1} \approx 2.7\ \mathrm{m}^{-1}$. For larger values of l_{coh}^{-1}, the difference in speckle contrast C_I between reference and cloak samples is evident from Figs. 2(b) and 2(c). This means that the cloak can indeed be revealed without having to measure the complete distributions of path lengths $P(s)$.

Finally, our experiments and the corresponding theory have considered the case of simplified core-shell cloaks. We have used a cylindrical geometry throughout this paper because the effects are more pronounced than for spherical geometry [11]. One might ask whether the conclusions drawn also apply for refined cloaks designed by spatial coordinate transformations [15], which can be approximated by cloaks composed of many layers [13]. The answer is yes, because the described uncloaking mechanism using partially coherent light builds upon the fact that the geometrical path-length distribution $P(s)$ or, equivalently, the propagation-time distribution, is significantly different for the reference and the cloak, respectively [15].

In conclusion, we have shown that diffusive-light invisibility cloaks can work well under stationary conditions in the limits of very small and very large coherence lengths of light, but can be uncloaked for the intermediate case of illumination with partially coherent light and inspection of the resulting speckle contrast. Broadly speaking, all types of cloaks have their Achilles' heels, and partial coherence is one for diffusive-light cloaking. The same weakness is, of course, expected for other diffusing-wave cloaks, e.g., in acoustics.

Funding. Deutsche Forschungsgemeinschaft (DFG) (DFG-SPP 1839 "Tailored Disorder"); Helmholtz-Gemeinschaft (HGF); Science and Technology of Nanosystems; Karlsruhe School of Optics and Photonics (KSOP); National Science Foundation (NSF) (DMR-1205223).

Acknowledgment. We thank Sylvain Gigan (Université Pierre et Marie Curie, France) and Aristide Dogariu (CREOL, USA) for insightful discussions. We thank the group of Heinz Kalt (KIT) for lending us the laser and Toptica for lending us the interferometer.

REFERENCES

1. M. Kadic, T. Bückmann, R. Schittny, and M. Wegener, Rep. Prog. Phys. **76**, 126501 (2013).
2. A. Greenleaf, M. Lassas, and G. Uhlmann, Math. Res. Lett. **10**, 685 (2003).
3. H. Hashemi, B. Zhang, J. D. Joannopoulos, and S. G. Johnson, Phys. Rev. Lett. **104**, 253903 (2010).
4. F. Monticone and A. Alù, Phys. Rev. X **3**, 041005 (2013).
5. F. Monticone and A. Alù, Optica **3**, 718 (2016).
6. B. Zhang and B. Wu, Phys. Rev. Lett. **103**, 243901 (2009).
7. J. C. Halimeh, R. T. Thompson, and M. Wegener, Phys. Rev. A **93**, 013850 (2016).
8. J. W. Goodman, *Speckle Phenomena in Optics: Theory and Applications* (Roberts & Company, 2007).
9. F. Martelli, S. D. Bianco, A. Ismaelli, and G. Zaccanti, *Light Propagation through Biological Tissue and Other Diffusive Media: Theory, Solutions, and Software* (SPIE, 2010).
10. S. Guenneau, C. Amra, and D. Veynante, Opt. Express **20**, 8207 (2012).
11. R. Schittny, M. Kadic, T. Bückmann, and M. Wegener, Science **345**, 427 (2014).
12. R. Schittny, A. Niemeyer, M. Kadic, T. Bückmann, A. Naber, and M. Wegener, Opt. Lett. **40**, 4202 (2015).
13. R. Schittny, A. Niemeyer, F. Mayer, A. Naber, M. Kadic, and M. Wegener, Laser Photon. Rev. **10**, 382 (2016).
14. F. Mayer, R. Schittny, A. Egel, A. Niemeyer, J. Preinfalk, U. Lemmer, and M. Wegener, Adv. Opt. Mater. **4**, 740 (2016).
15. R. Schittny, A. Niemeyer, M. Kadic, T. Bückmann, A. Naber, and M. Wegener, Optica **2**, 84 (2015).
16. B. Orazbayev, M. Beruete, A. Martínez, and C. García-Meca, Phys. Rev. A **94**, 063850 (2016).
17. M. Farhat, P. Y. Chen, S. Guenneau, H. Bağcı, K. N. Salama, and A. Alù, Proc. R. Soc. A **472**, 20160276 (2016).
18. M. Koirala and A. Yamilov, Opt. Lett. **41**, 3860 (2016).
19. M. C. W. van Rossum and T. M. Nieuwenhuizen, Rev. Mod. Phys. **71**, 313 (1999).
20. G. Popescu and A. Dogariu, Opt. Lett. **24**, 442 (1999).
21. C. A. Thompson, K. J. Webb, and A. M. Weiner, Appl. Opt. **36**, 3726 (1997).
22. J. D. McKinney, M. A. Webster, K. J. Webb, and A. M. Weiner, Opt. Lett. **25**, 4 (2000).
23. N. Curry, P. Bondareff, M. Leclercq, N. F. Van Hulst, R. Sapienza, S. Gigan, and S. Grésillon, Opt. Lett. **36**, 3332 (2011).
24. A. Dogariu and R. Carminati, Phys. Rep. **559**, 1 (2015).
25. D. A. Boas and A. K. Dunn, J. Biomed. Opt. **15**, 011109 (2010).
26. R. B. Bird, W. E. Stewart, and E. N. Lightfoot, *Transport Phenomena* (Wiley, 1960).